SIAM J. Applied Dynamical Systems
Vol. 2, No. 3, pp. 277–296

Synergetic System Analysis for the Delay-Induced Hopf Bifurcation in the Wright Equation*

Michael Schanz† and Axel Pelster‡

Abstract. We apply the synergetic elimination procedure for the stable modes in nonlinear delay systems close to a dynamical instability and derive the normal form for the delay-induced Hopf bifurcation in the Wright equation. The resulting periodic orbit is confirmed by numerical simulations.

Key words. delay-induced bifurcations, normal forms, center manifold theory, synergetics

AMS subject classifications. 34K17, 37G10, 37L10

DOI. 10.1137/S1111111102412802

1. Introduction.

Within the last decades, synergetics has provided powerful concepts and methods to describe self-organization processes in various branches of science [1, 2, 3, 4, 5, 6]. The spontaneous formation of spatial, temporal, or functional patterns in complex systems has been successfully investigated by working out general principles and by mapping them onto universal mathematical structures. The important result is due to the fact that in the vicinity of a dynamical instability the high-dimensional set of nonlinear evolution equations modeling a complex system on a microscopic or a mesoscopic scale can approximately be reduced to a low-dimensional set of order parameter equations describing the evolving pattern formation on a macroscopic scale. To obtain such a simplified, reduced description of self-organization processes, the synergetic system analysis proceeds as follows. A linearization of the evolution equations around a stationary solution shows that a dynamical instability is always accompanied by a time-scale hierarchy between numerous fast modes s and few slow modes u. A rigorous treatment of the full nonlinear evolution equations in the vicinity of the dynamical instability leads to a characteristic interdependence between both hierarchy levels which may be illustrated by a circular causality chain. On the one hand, the slaving principle of synergetics states that the numerous fast modes s quasi-instantaneously take values which are prescribed by the few slow modes u according to $s(t) = h(u(t))$ with the center manifold $h(u)$. On the other hand, an adiabatic elimination of the fast enslaved modes s yields equations for the slow order parameters u which depend, in general, on the center manifold $h(u)$ due to the nonlinear feedback.

In its original formulation, the synergetic system analysis was developed for complex systems which can be modeled by ordinary and partial differential equations as well as their

*Received by the editors August 8, 2002; accepted for publication (in revised form) by R. Murray January 21, 2003; published electronically August 15, 2003.
http://www.siam.org/journals/siads/2-3/41280.html

†Institute of Parallel and Distributed Systems, University of Stuttgart, Breitwiesenstraße 20-22, D-70565 Stuttgart, Germany (Michael.Schanz@informatik.uni-stuttgart.de).
‡Institute of Theoretical Physics, Free University of Berlin, Arnimallee 14, D-14195 Berlin, Germany (pelster@physik.fu-berlin.de).

stochastic generalizations. Some time ago, the general concepts and methods of synergetics were extended to delay differential equations to deal with dynamical instabilities which are induced by the finite propagation time of signals in feedback loops [7]. Taking into account the infinite-dimensional character of a delay system [8, 9], the adiabatic elimination of the stable modes leads to a low-dimensional set of order parameter equations which turn out to be of the form of ordinary differential equations; i.e., they no longer contain memory effects. The predictions of the synergetic system analysis have been quantitatively tested by investigating the delay-induced Hopf bifurcation of the electronic system of a first-order phase-locked loop (PLL) [7]. The periodic orbit which results from the corresponding order parameter equation near the bifurcation point has been confirmed by both a multiple scale procedure and numerical simulations [10, 11]. Although this application exemplarily proves the order parameter concept for delay systems, it does not allow us to draw conclusions about the slaving principle. As the lowest nonlinear term in the scalar delay differential equation of the PLL is a cubic one, the center manifold does not influence the order parameter equation of the Hopf bifurcation in the lowest order. In order to check both ingredients of the circular causality chain, i.e., the order parameter concept and the slaving principle, for delay systems, it is thus indispensable to study a scalar delay differential equation with a quadratic nonlinearity. Such dynamical systems were studied, for instance, in the context of Lotka–Volterra models [12] and machining models [13, 14].

Another candidate is provided by the evolution equation

$$\frac{d}{dt}z(t) = R\left[z(t) - z(t-\tau)^2\right]. \tag{1.1}$$

With vanishing time delay τ, it represents a system which is named after the Belgian mathematician P. F. Verhulst from the 19th century [15]. It is used as a simplified model for the population dynamics of a species in an environment with limited food supply [16]. The synergetic system analysis for the Verhulst system with time delay (1.1) has already been performed in [10]. There also the well-known equation of Wright [17]

$$\frac{d}{dt}z(t) = -Rz(t-\tau)\left[1 + z(t)\right] \tag{1.2}$$

has been treated, where R denotes a system parameter and τ a delay time. This delay differential equation is mentioned by Wright [17] as arising in the application of probability methods to the theory of asymptotic prime number density. Cunningham [18] depicts it as a "growth equation" representing a mathematical description of a fluctuating population of organisms under certain environmental conditions. In addition, it may describe the operation of a control system working with potentially explosive chemical reactions. Performing an appropriate scaling of time

$$t = \tau\, t', \quad z'(t') = z(\tau\, t') \tag{1.3}$$

converts the Wright equation (1.2) to its standard form with the control parameter

$$R' = \tau\, R. \tag{1.4}$$

Thus varying the delay time τ corresponds to changing the control parameter R'. By omitting the prime $'$ for the respective quantities, the standard form of the Wright equation reads

$$\frac{d}{dt}z(t) = -Rz(t-1)\,[1+z(t)]\,. \tag{1.5}$$

In this paper, we restrict ourselves to analyzing this standard form of the Wright equation.

The Wright equation (1.5) shows a delay-induced instability, namely, a Poincaré–Andronov–Hopf bifurcation at the critical value

$$R_c = \frac{\pi}{2} \tag{1.6}$$

of the control parameter R. In [19], it is shown that the oscillatory solution in the vicinity of this instability, i.e., the emerging limit cycle, can be calculated approximately using the method of *averaging*. This approximation reads in the lowest order

$$z(t) = A\sqrt{R-\frac{\pi}{2}}\,\cos\left(\frac{\pi}{2}t\right) + \mathcal{O}\left(R-\frac{\pi}{2}\right), \tag{1.7}$$

where the amplitude A has the value

$$A = \sqrt{\frac{40}{3\pi-2}}. \tag{1.8}$$

In section 2, we start with a linear stability analysis of the Wright equation (1.5) which confirms, of course, the delay-induced Poincaré–Andronov–Hopf bifurcation when the control parameter R approaches the critical value (1.6). Near this instability, we perform a nonlinear synergetic treatment in section 3 and study in detail how the center manifold influences the order parameter equation. In section 4, the resulting order parameter equation is transformed to the normal form of a Hopf bifurcation, where the emerging periodic orbit is determined one order higher than the lowest-order result (1.7) and (1.8). The numerical investigations of section 5 confirm the emerging periodic orbit; furthermore, we discuss the global bifurcation scenario of the Wright equation (1.5).

2. Linear stability analysis. The solution of the delay differential equation (1.5) for times $t \geq 0$ depends on the initial values of the function $z(t)$ in the entire interval $[-1,0]$. In order to properly define such an initial value problem, Hale [8] and Krasovskii [9] proposed to transform the equation of motion (1.5) for a function $z(t)$ in the usual state space Γ to the extended state space $\mathcal{C}$ of continuous complex valued functions z_t, which are defined on the interval $[-1,0]$:

$$\frac{d}{dt}z_t(\Theta) = (\mathcal{G}\,z_t)\,(\Theta) = \begin{cases} \dfrac{d}{d\Theta}z_t(\Theta), & -1 \leq \Theta < 0, \\ \mathcal{F}[z_t], & \Theta = 0. \end{cases} \tag{2.1}$$

Following the notation of [7], we introduced not only the new function $z_t \in \mathcal{C}$, which is connected to the original function $z(t) \in \Gamma$ through

$$z_t(\Theta) = z(t+\Theta)\,, \quad -1 \leq \Theta \leq 0, \tag{2.2}$$

but also the nonlinear functional

$$\mathcal{F}[z_t] = \sum_{k=1}^{2} \int_{-1}^{0} d\Theta_1 \cdots \int_{-1}^{0} d\Theta_k \, \omega^{(k)}(\Theta_1, \ldots, \Theta_k) \prod_{l=1}^{k} z_t(\Theta_l) \tag{2.3}$$

with the two scalar densities

$$\omega^{(1)}(\Theta_1) = -R\boldsymbol{\delta}(\Theta_1 + 1), \tag{2.4}$$

$$\omega^{(2)}(\Theta_1, \Theta_2) = -R\boldsymbol{\delta}(\Theta_1 + 1)\boldsymbol{\delta}(\Theta_2). \tag{2.5}$$

The stationary states of this system

$$z^{\mathrm{I}}_{\mathrm{stat}} = 0\,, \qquad z^{\mathrm{II}}_{\mathrm{stat}} = -1 \tag{2.6}$$

are candidates for the reference state from which we start our further investigations. For the main body of the article, we focus our attention on the stationary state $z^{\mathrm{I}}_{\mathrm{stat}}$ and choose it as the reference state. The other stationary state $z^{\mathrm{II}}_{\mathrm{stat}}$ will be discussed in section 5 together with the global bifurcation scenario of the Wright equation (1.5).

Then we linearize the system (2.1) with respect to the stationary state $z^{\mathrm{I}}_{\mathrm{stat}} = 0$ by using the decomposition

$$z_t(\Theta) = z^{\mathrm{I}}_{\mathrm{stat}} + \zeta_t(\Theta)\,, \quad -1 \le \Theta \le 0. \tag{2.7}$$

This leads to the following linearized equation of motion for the deviation $\zeta_t(\Theta)$ from the stationary state $z^{\mathrm{I}}_{\mathrm{stat}} = 0$:

$$\frac{d}{dt}\zeta_t(\Theta) = (\mathcal{G}_L\,\zeta_t)\,(\Theta) = \begin{cases} \dfrac{d}{d\Theta}\zeta_t(\Theta), & -1 \le \Theta < 0, \\ \mathcal{L}[\zeta_t], & \Theta = 0, \end{cases} \tag{2.8}$$

where the linear functional is given by

$$\mathcal{L}\,[\zeta_t] = \int_{-1}^{0} d\Theta\, \omega(\Theta)\zeta_t(\Theta) \tag{2.9}$$

with the scalar density

$$\omega(\Theta) = \left.\frac{\delta\mathcal{F}[z_t]}{\delta z_t(\Theta)}\right|_{z_t(\Theta)=z^{\mathrm{I}}_{\mathrm{stat}}} = -R\,\boldsymbol{\delta}(\Theta + 1). \tag{2.10}$$

Inserting the solution ansatz

$$\zeta_t(\Theta) = \phi^{\lambda}(\Theta)e^{\lambda t}, \quad -1 \le \Theta \le 0, \tag{2.11}$$

into (2.8) leads to the eigenvalue problem of the infinitesimal generator $\mathcal{G}_L$:

$$\lambda\phi^{\lambda}(\Theta) = \left(\mathcal{G}_L\phi^{\lambda}\right)(\Theta), \quad -1 \le \Theta \le 0. \tag{2.12}$$

Taking into account the definition of $\mathcal{G}_L$ in (2.8), the eigenfunction $\phi^\lambda(\Theta)$ is determined to be

$$\phi^\lambda(\Theta) = N_\lambda e^{\lambda\Theta}, \quad -1 \le \Theta \le 0, \tag{2.13}$$

and the eigenvalue λ follows from

$$\lambda = L(\lambda), \tag{2.14}$$

where $L(\lambda)$ is defined by

$$L(\lambda) = \int_{-1}^{0} d\Theta\, \omega(\Theta) e^{\lambda\Theta}. \tag{2.15}$$

Using the scalar density (2.10), we obtain the following transcendental characteristic equation:

$$-Re^{-\lambda} - \lambda = 0. \tag{2.16}$$

Thus the spectrum of the linear operator $\mathcal{G}_L$ has the following properties [8]:

- It consists of a countable infinite number of eigenvalues which cumulate for $\Re(\lambda) \to -\infty$.
- It is confined by an upper threshold for the real parts of the eigenvalues.
- At the bifurcation point, i.e., the instability, some of the eigenvalues reach the imaginary axes and thus become unstable.

Further properties of the eigenvalues of the characteristic equation (2.16) follow from the Hayes theorem, which can be found in [20]. It states that all solutions of the transcendental equation

$$p + qe^{-\lambda} - \lambda = 0 \tag{2.17}$$

possess a negative real part if and only if (a) $p < 1$ and (b) $p < -q < \sqrt{a_1^2 + p^2}$. Here a_1 represents the solution of the transcendental equation $a_1 = p\tan(a_1)$ which lies in the interval $[0, \pi)$. For the special case $p = 0$, one can show that a_1 is equal to $\pi/2$. The shaded region in Figure 2.1 represents that region of the parameter space q, p where both conditions of the Hayes theorem are fulfilled. The upper boundary line stems from (a) $p < 1$ and (b1) $p < -q$, whereas the lower boundary line follows from (a) $p < 1$ and (b2) $-q < \sqrt{a_1^2 + p^2}$.

Comparing (2.16) with (2.17), we obtain the identification $q = -R$ and $p = 0$. Changing the control parameter R from 0 to $\pi/2$, the corresponding point in the parameter space q, p moves along the q-axis from the point $q = 0$ to $q = -\pi/2$ (see the arrow in Figure 2.1). At this critical value, it reaches the boundary of the shaded stability region; i.e., no longer do all solutions of the characteristic equation (2.16) have a negative real part. Therefore, an instability occurs at $R_c = \pi/2$.

Figure 2.2 confirms this result by illustrating the movement of the ten solutions of the characteristic equation (2.16) with the largest real part when the control parameter is increased from 0 to $\pi/2$. The eigenvalues were obtained with a Newton algorithm, and the control parameter R was increased in equidistant steps. For $R = 0$, there exists only one

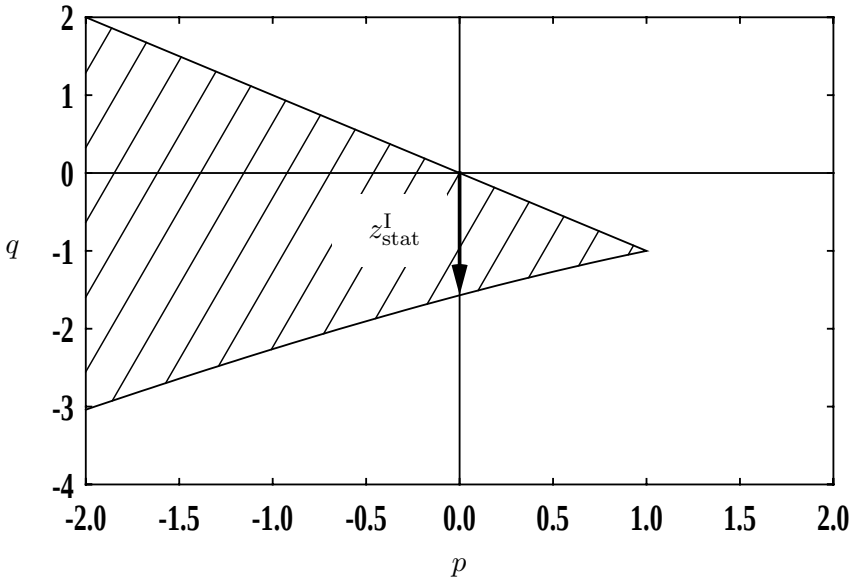

Figure 2.1. *The Hayes theorem is fulfilled within the shaded region.*

real eigenvalue 0 as the linearized delay differential equation (2.8) degenerates to an ordinary differential equation. For $R > 0$, this eigenvalue remains real and becomes negative. Furthermore, a countable infinite number of conjugate complex eigenvalues and another real eigenvalue emerge from an infinite negative real part. At the value $R = 1/e$, both real eigenvalues meet at the point $(-1/0)$. They are converted to a pair of conjugated complex eigenvalues for $1/e < R < \pi/2$. These two complex conjugated eigenvalues have zero real part at the instability $R_c = \pi/2$, which thus represents a Hopf bifurcation. We can further analyze this instability by introducing the smallness parameter

$$\varepsilon = \frac{R - R_c}{R_c} \quad \Longleftrightarrow \quad R = R_c(1 + \varepsilon) \tag{2.18}$$

for the deviation from the critical control parameter $R_c = \pi/2$. In particular, we can determine both eigenvalues $\lambda_u^{\pm}(\varepsilon)$ with nearly vanishing real part at $\varepsilon \approx 0$ from the characteristic equation (2.16):

$$\lambda_u^{\pm}(\varepsilon) = \frac{R_c^2}{1 + R_c^2}\,\varepsilon \pm i R_c \left(1 + \frac{1}{1 + R_c^2}\,\varepsilon\right) + \mathcal{O}\left(\varepsilon^2\right). \tag{2.19}$$

In the vicinity of the instability $\varepsilon \approx 0$, we read off from Figure 2.2 that only the two eigenvalues (2.19) have nearly vanishing real part; all other eigenvalues have a large negative real part:

$$\Re[\lambda_u^{\pm}(\varepsilon \approx 0)] \approx 0; \quad \Re[\lambda_s^{j}(\varepsilon \approx 0)] < 0, \quad j = 1, \ldots, \infty. \tag{2.20}$$

This characteristic property of the linearized system (2.8) leads to the time-scale hierarchy

$$T_u^{\pm} = \frac{1}{\Re[\lambda_u^{\pm}(\varepsilon \approx 0)]} \gg T_s^{j} = \frac{1}{\Re[\lambda_s^{j}(\varepsilon \approx 0)]}, \quad j = 1, \ldots, \infty. \tag{2.21}$$

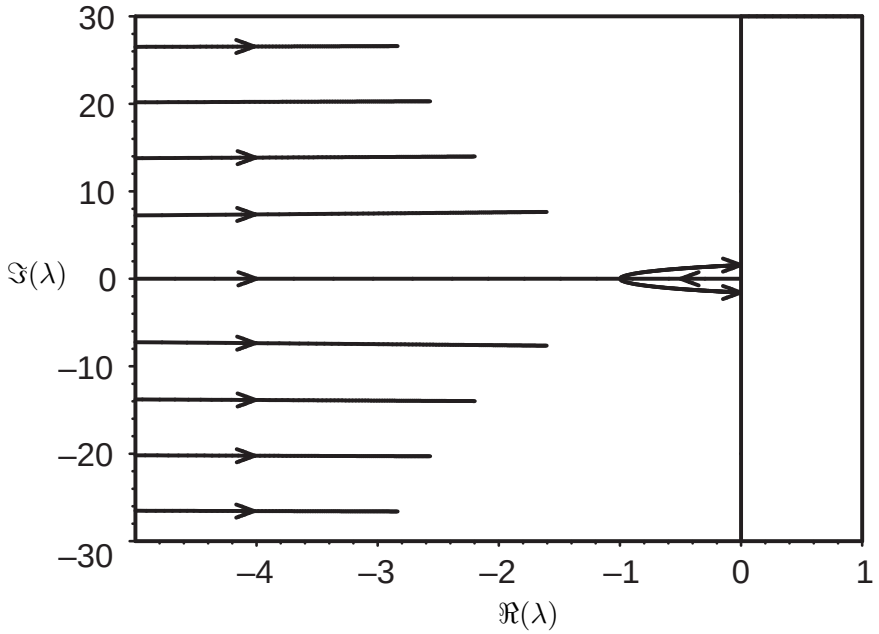

Figure 2.2. *Movement of the ten solutions of the characteristic equation* (2.16) *with the largest real part.*

Thus the infinite-dimensional extended state space $\mathcal{C}$ decomposes in a two-dimensional subspace $\mathcal{U}$ of the linear unstable modes and a remaining infinite-dimensional subspace $\mathcal{S}$ of the linear stable modes [7]. As a consequence, the extended state function z_t can be decomposed near the instability according to

$$z_t(\Theta) = z_{\text{stat}}^{\text{I}} + u_t(\Theta) + s_t(\Theta) = u_t(\Theta) + s_t(\Theta), \quad -1 \leq \Theta \leq 0, \tag{2.22}$$

as we have $z_{\text{stat}}^{\text{I}} = 0$. Here u_t and s_t denote the respective contributions of z_t in the subspaces $\mathcal{U}$ and $\mathcal{S}$. In order to project into these subspaces, we need the linear unstable modes

$$\phi^{\lambda_u^{\pm}}(\Theta) = N_{\lambda_u^{\pm}} e^{\lambda_u^{\pm}\Theta}, \quad -1 \leq \Theta \leq 0, \tag{2.23}$$

of the system (2.8) which have already been determined in (2.13). However, this knowledge is not sufficient, as the infinitesimal generator $\mathcal{G}_L$ is not self-adjoint. Therefore, we also need the linear unstable modes

$$\psi^{\dagger\lambda_u^{\pm}}(s) = N_{\lambda_u^{\pm}} e^{-\lambda_u^{\pm} s}, \quad 0 \leq s \leq 1, \tag{2.24}$$

of the adjoint system

$$\frac{d}{dt}\zeta_t^{\dagger}(s) = -\left(\mathcal{G}_L^{\dagger}\,\zeta_t^{\dagger}\right)(s) = \begin{cases} \dfrac{d}{ds}\zeta_t^{\dagger}(s), & 0 < s \leq 1, \\ -\mathcal{L}^{\dagger}[\zeta_t^{\dagger}], & s = 0, \end{cases} \tag{2.25}$$

where the linear functional

$$\mathcal{L}^{\dagger}\left[\zeta_t^{\dagger}\right] = \int_0^1 ds\, \omega(-s)\zeta_t^{\dagger}(s) \tag{2.26}$$

also contains the scalar density (2.10). Indeed, the solution ansatz

$$\zeta_t^\dagger(s) = \psi^{\dagger\lambda}(s)e^{-\lambda s}, \quad 0 \le s \le 1, \tag{2.27}$$

converts (2.25) to the eigenvalue problem

$$\lambda\psi^{\dagger\lambda}(s) = \left(\mathcal{G}_L^\dagger \psi^{\dagger\lambda}\right)(s), \quad 0 \le s \le 1, \tag{2.28}$$

which is adjoint to (2.12). Note that $\psi^{\dagger\lambda}$ and $\zeta_t^\dagger$ are elements of the dual extended state space $\mathcal{C}^\dagger$, which consists of continuous complex valued functions on the interval $[0,1]$. The relation between both extended state spaces $\mathcal{C}$ and $\mathcal{C}^\dagger$ is defined by the bilinear form [7]

$$\left(\psi^\dagger|\phi\right) = \psi^\dagger(0)\phi(0) - \int_{-1}^{0} d\Theta \int_0^\Theta ds\, \psi^\dagger(s-\Theta)\omega(\Theta)\phi(s). \tag{2.29}$$

Using this bilinear form, one can show that the eigenfunctions (2.23) and (2.24) are biorthonormal:

$$\left(\psi^{\dagger\lambda_i}|\phi^{\lambda_j}\right) = \delta_{ij}, \quad i,j = \pm. \tag{2.30}$$

This determines the yet unknown normalization constants to be

$$N_{\lambda_u^\pm} = \frac{1}{\sqrt{1+\lambda_u^\pm}}, \tag{2.31}$$

so they reduce near the instability because of (2.19) to

$$N_{\lambda_u^\pm} = \frac{1}{\sqrt{1 \pm iR_c}} + \mathcal{O}(\varepsilon). \tag{2.32}$$

Furthermore, the bilinear form (2.29) allows us to define the projector into the two-dimensional subspace $\mathcal{U}$ of the unstable modes:

$$\left(\mathcal{P}_u \bullet\right)(\Theta) = \sum_{i=\pm} \phi^{\lambda_u^i}(\Theta)\left(\psi^{\dagger\lambda_u^i}\middle|\bullet\right). \tag{2.33}$$

Correspondingly, the projector into the remaining infinite-dimensional subspace $\mathcal{S}$ of the stable modes reads

$$\mathcal{P}_s \bullet = (\mathcal{I} - \mathcal{P}_u)\bullet. \tag{2.34}$$

Applying the projector $\mathcal{P}_u$ to $z_t \in \mathcal{C}$ leads to $u_t \in \mathcal{U}$ according to

$$u_t(\Theta) = \left(\mathcal{P}_u z_t\right)(\Theta) = \sum_{i=\pm} u^i(t)\phi^{\lambda_u^i}(\Theta), \quad -1 \le \Theta \le 0, \tag{2.35}$$

where the amplitudes of the linear unstable modes $\phi^{\lambda_u^\pm}(\Theta)$ are defined by

$$u^\pm(t) = \left(\psi^{\dagger\lambda_u^\pm}\middle|\, z_t\right). \tag{2.36}$$

Later on, these amplitudes represent the order parameters which indicate the emergence of an instability. Analogously, the projector (2.34) leads to the stable modes

$$s_t(\Theta) = \left(\mathcal{P}_s z_t\right)(\Theta), \quad -1 \le \Theta \le 0. \tag{2.37}$$

3. Nonlinear synergetic analysis. After having performed a linear stability analysis around the reference state $z^{\mathrm{I}}_{\mathrm{stat}} = 0$ in the vicinity of the instability $R_c = \pi/2$, we now return to our original nonlinear evolution equation (2.1) in the extended state space $\mathcal{C}$. We proceed by decomposing the generator $\mathcal{G}$ into its linear part $\mathcal{G}_L$ and a remaining effective nonlinear part:

$$\frac{d}{dt} z_t(\Theta) = \left(\mathcal{G}_L\, z_t\right)(\Theta) + X_0(\Theta)\mathcal{F}^{\mathrm{eff}}[z_t], \quad -1 \le \Theta \le 0. \tag{3.1}$$

Here we introduce the scalar function

$$X_0(\Theta) = \begin{cases} 0, & -1 \le \Theta < 0, \\ 1, & \Theta = 0, \end{cases} \tag{3.2}$$

and the effective nonlinear functional

$$\mathcal{F}^{\mathrm{eff}}[z_t] = \int_{-1}^{0} d\Theta_1 \int_{-1}^{0} d\Theta_2\, \omega^{(2)}(\Theta_1, \Theta_2)\, z_t(\Theta_1) z_t(\Theta_2) \tag{3.3}$$

with the scalar density (2.5). Using the projectors (2.33) and (2.34) and their properties (2.35)–(2.37), we can investigate the respective contributions of the order parameters $u^{\pm}(t)$ and the linear stable modes $s_t \in \mathcal{S}$ to the nonlinear dynamics (3.1). Thus we obtain the following system of coupled nonlinear mode equations:

$$\frac{d}{dt} u^{\pm}(t) = \lambda^{\pm}_u u^{\pm}(t) + \psi^{\dagger\lambda^{\pm}_u}(0)\, \mathcal{F}^{\mathrm{eff}}\left[\sum_{j=\pm} \phi^{\lambda^j_u} u^j(t) + s_t\right], \tag{3.4}$$

$$\frac{d}{dt} s_t(\Theta) = \left(\mathcal{G}_L s_t\right)(\Theta) + \left(\left(\mathcal{I} - \mathcal{P}_u\right) X_0\right)(\Theta)\, \mathcal{F}^{\mathrm{eff}}\left[\sum_{j=\pm} \phi^{\lambda^j_u} u^j(t) + s_t\right]. \tag{3.5}$$

It is still exact and describes completely the nonlinear dynamics. However, a solution to these equations can only be found by means of an approximation method. Such a well-established approximative solution is provided by the slaving principle of synergetics [1, 2, 3, 4, 5].

To this end, we start with the time-scale hierarchy (2.21) near the instability which leads to the fact that the dynamics of the stable modes $s_t \in \mathcal{S}$ evolves much faster than the order parameters $u^{\pm}(t)$. In [7] it has been shown for a quite general class of delay differential equations that such a time-scale hierarchy leads to a slaving of the stable modes; i.e., the numerous fast modes $s_t \in \mathcal{S}$ quasi-instantaneously take values which are prescribed by the few slow order parameters $u^{\pm}(t)$. In our context, the slaving principle states mathematically that the dynamics of the stables modes $s_t \in \mathcal{S}$ is determined by the center manifold $h(\Theta, u^+, u^-)$ according to

$$s_t(\Theta) = h\left(\Theta, u^+(t), u^-(t)\right). \tag{3.6}$$

Inserting this ansatz into (3.5) leads to an implicit equation for the center manifold $h(\Theta, u^+, u^-)$:

$$\begin{aligned} \sum_{i=\pm} \frac{\partial h\left(\Theta, u^+(t), u^-(t)\right)}{\partial u^i(t)} \left(\lambda^i_u u^i(t) + \psi^{\dagger\lambda^i_u}(0)\ \mathcal{F}^{\mathrm{eff}}\left[\sum_{j=\pm} \phi^{\lambda^j_u} u^j(t) + h\right]\right) \\ = \left(\mathcal{G}_L h\right)(\Theta) + \left(\left(\mathcal{I} - \mathcal{P}_u\right) X_0\right)(\Theta)\, \mathcal{F}^{\mathrm{eff}}\left[\sum_{j=\pm} \phi^{\lambda^j_u} u^j(t) + h\right]. \end{aligned} \tag{3.7}$$

It can be approximately solved in the vicinity of the instability as follows. We assume that the order parameters $u^{\pm}(t)$ possess a certain dependence on the smallness parameter (2.18) which is typical for a Hopf bifurcation:

$$u^{\pm}(t) = \mathcal{O}(\varepsilon^{1/2}). \tag{3.8}$$

Furthermore, we perform for the center manifold $h(\Theta, u^+, u^-)$ the lowest-order ansatz

$$h(\Theta, u^+, u^-) = \sum_{j_1=\pm} \sum_{j_2=\pm} H_{j_1 j_2}(\Theta) u^{j_1}(t) u^{j_2}(t), \tag{3.9}$$

as $r = 2$ is the order of the effective nonlinear functional (3.3). From (3.8) and (3.9), it follows then in lowest order of ε that the effective nonlinear functional $\mathcal{F}^{\text{eff}}$ in (3.7) can be approximated by

$$\mathcal{F}^{\text{eff}}\left[\sum_{j=\pm} \phi^{\lambda_u^j} u^j(t) + h\right] \approx \sum_{j_1=\pm} \sum_{j_2=\pm} F^{\text{eff}}_{j_1 j_2} u^{j_1}(t) u^{j_2}(t), \tag{3.10}$$

where the coefficients $F^{\text{eff}}_{j_1 j_2}$ read

$$F^{\text{eff}}_{j_1 j_2} = \int_{-1}^{0} d\Theta_1 \int_{-1}^{0} d\Theta_2 \, \omega^{(2)}(\Theta_1, \Theta_2) \, \phi^{\lambda_u^{j_1}}(\Theta_1) \phi^{\lambda_u^{j_2}}(\Theta_2). \tag{3.11}$$

Taking into account (2.5) and (2.23), these coefficients turn out to be

$$F^{\text{eff}}_{++} = F^{\text{eff}\,*}_{--} = -RN^2_{\lambda_u^+} e^{-\lambda_u^+}, \quad F^{\text{eff}}_{+-} = F^{\text{eff}}_{-+} = -RN_{\lambda_u^+} N_{\lambda_u^-} e^{-\lambda_u^+}. \tag{3.12}$$

As a consequence, we conclude from (3.7) in lowest order of ε that the coefficients $H_{j_1 j_2}(\Theta)$ of the center manifold (3.9) are given by

$$H_{j_1 j_2}(\Theta) = F^{\text{eff}}_{j_1 j_2} K_{j_1 j_2}(\Theta), \tag{3.13}$$

where the coefficients $K_{j_1 j_2}(\Theta)$ follow from

$$K_{j_1 j_2}(\Theta) = \left([\mathcal{G}_L - \Lambda]^{-1} (\mathcal{P}_u X_0 - X_0) \right)(\Theta) \tag{3.14}$$

with the abbreviation

$$\Lambda = \sum_{k=1}^{2} \lambda_u^{j_k}. \tag{3.15}$$

In [7] it is shown that the operator $[\mathcal{G}_L - \Lambda]^{-1}$ has the explicit representation

$$\begin{aligned} \left([\mathcal{G}_L - \Lambda]^{-1} \chi \right)(\Theta) &= \int_0^{\Theta} ds \, e^{\Lambda(\Theta - s)} \chi(s) \\ &+ [L(\Lambda) - \Lambda]^{-1} \left(\chi(0) - \int_{-1}^{0} d\Theta \int_0^{\Theta} ds \, e^{\Lambda(\Theta - s)} \omega(\Theta) \chi(s) \right) e^{\Lambda \Theta}, \end{aligned} \tag{3.16}$$

where $L(\lambda)$ is already defined in (2.15). After some calculation, which also involves (2.10), (2.23), (2.24), (2.33), and (3.2), it thus follows that the coefficients (3.14) are given by

$$K_{j_1 j_2}(\Theta) = \sum_{j=\pm} \frac{N^2_{\lambda_u^j}}{\lambda_u^j - \Lambda} e^{\lambda_u^j \Theta} - \frac{e^{\Lambda\Theta}}{L(\Lambda) - \Lambda}. \tag{3.17}$$

Thus, together with (2.10), (2.15), and (3.15), we obtain

$$K_{++}(\Theta) = K^*_{--}(\Theta) = -\frac{N^2_{\lambda_u^+} e^{\lambda_u^+ \Theta}}{\lambda_u^+} + \frac{N^2_{\lambda_u^-} e^{\lambda_u^- \Theta}}{\lambda_u^- - 2\lambda_u^+} + \frac{e^{2\lambda_u^+ \Theta}}{Re^{-2\lambda_u^+} + 2\lambda_u^+}, \tag{3.18}$$

$$K_{+-}(\Theta) = K_{-+}(\Theta) = -\frac{N^2_{\lambda_u^+} e^{\lambda_u^+ \Theta}}{\lambda_u^-} - \frac{N^2_{\lambda_u^-} e^{\lambda_u^- \Theta}}{\lambda_u^+} + \frac{e^{(\lambda_u^+ + \lambda_u^-)\Theta}}{Re^{-(\lambda_u^+ + \lambda_u^-)} + \lambda_u^+ + \lambda_u^-}. \tag{3.19}$$

This completes the lowest-order result for the center manifold $h(\Theta, u^+, u^-)$, which is given by (3.9), (3.12), (3.13), (3.18), and (3.19).

Thus we can now consider the order parameter equation (3.4). In lowest order in ε we take into account (2.5), (2.25), (3.3), (3.6), and (3.9) so that it reduces to

$$\begin{aligned} \frac{d}{dt} u^\pm(t) &= \lambda_u^\pm u^\pm(t) \\ &- R N_{\lambda_u^\pm} \prod_{l=1}^{2} \left[\sum_{j=\pm} \phi^{\lambda_u^j}(\vartheta_l) u^j(t) + \sum_{j_1=\pm} \sum_{j_2=\pm} H_{j_1 j_2}(\vartheta_l) u^{j_1}(t) u^{j_2}(t) \right], \end{aligned} \tag{3.20}$$

where we set

$$\vartheta_l = \begin{cases} -1, & l = 1, \\ 0, & l = 2. \end{cases} \tag{3.21}$$

Note that the order parameter equation (3.20) turns out to be an ordinary differential equation; i.e., it no longer contains memory effects. Furthermore, we observe that the center manifold explicitly enters the order parameter equation (3.20) as a direct consequence of the quadratic nonlinearity of the Wright equation (1.5). We remark that this effect, which is essential for the present synergetic analysis, was neglected in the neurophysiological study in [23]. In the subsequent section we show how the order parameter equation (3.20) is converted to the normal form of a Hopf bifurcation.

4. Normal form. Now we perform a nonlinear transformation of the order parameters which eliminates those terms which are irrelevant for the normal form of a Hopf bifurcation. As far as the so-called *near identity transformation* and the theory of normal forms in general is concerned, we refer to the [19, 21, 22]. The terms in (3.20) which are relevant for the normal form of a Hopf bifurcation read

$$\frac{d}{dt} u^\pm(t) = \lambda_u^\pm u^\pm(t) + q_0^\pm u^\pm(t)^2 + q_1^\pm u^\pm(t) u^\mp(t) + q_2^\pm u^\mp(t)^2 + k_1^\pm u^\pm(t)^2 u^\mp(t) \tag{4.1}$$

as we can neglect quartic terms and nonresonant cubic terms due to the rotating wave approximation. The respective coefficients in (4.1) are given by

$$q_0^{\pm} = -RN_{\lambda_u^{\pm}}\phi^{\lambda_u^{\pm}}(-1)\phi^{\lambda_u^{\pm}}(0) = -RN_{\lambda_u^{\pm}}{}^3 e^{-\lambda_u^{\pm}}, \tag{4.2}$$

$$\begin{aligned} q_1^{\pm} &= -RN_{\lambda_u^{\pm}}\left[\phi^{\lambda_u^{\pm}}(-1)\phi^{\lambda_u^{\mp}}(0) + \phi^{\lambda_u^{\pm}}(0)\phi^{\lambda_u^{\mp}}(-1)\right] \\ &= -RN_{\lambda_u^{\pm}}{}^2 N_{\lambda_u^{\mp}}\left(e^{-\lambda_u^{\pm}} + e^{-\lambda_u^{\mp}}\right), \end{aligned} \tag{4.3}$$

$$q_2^{\pm} = -RN_{\lambda_u^{\pm}}\phi^{\lambda_u^{\mp}}(-1)\phi^{\lambda_u^{\mp}}(0) = -RN_{\lambda_u^{\pm}}N_{\lambda_u^{\mp}}{}^2 e^{-\lambda_u^{\mp}}, \tag{4.4}$$

$$\begin{aligned} k_1^{\pm} = -RN_{\lambda_u^{\pm}}\Big\{&\phi^{\lambda_u^{\pm}}(-1)\left[H_{+-}(0) + H_{-+}(0)\right] + \phi^{\lambda_u^{\mp}}(-1)H_{++}(0) \\ &+ \phi^{\lambda_u^{\pm}}(0)\left[H_{+-}(-1) + H_{-+}(-1)\right] + \phi^{\lambda_u^{\mp}}(0)H_{++}(-1)\Big\}, \end{aligned} \tag{4.5}$$

where we did not write down the explicit form of $k_1^{\pm}$ for simplicity. Then the previous order parameters $u^{\pm}(t)$ are transformed to new order parameters $v^{\pm}(t)$ by the near identity transformation

$$u^{\pm}(t) = v^{\pm}(t) + \alpha_0^{\pm}v^{\pm}(t)^2 + \alpha_1^{\pm}v^{\pm}(t)v^{\mp}(t) + \alpha_2^{\pm}v^{\mp}(t)^2, \tag{4.6}$$

with the yet-unknown coefficients $\alpha_0^{\pm}$, $\alpha_1^{\pm}$, and $\alpha_2^{\pm}$. As the $u^{\pm}(t)$ are small quantities in the vicinity of the instability, the same holds for the $v^{\pm}(t)$. Inserting (4.6) in (4.1), we obtain a system of ordinary differential equations of the form

$$M(t)\frac{d}{dt}\begin{pmatrix} v^+(t) \\ v^-(t) \end{pmatrix} = \begin{pmatrix} w^+(t) \\ w^-(t) \end{pmatrix}, \tag{4.7}$$

where the matrix $M(t)$ is defined by

$$M(t) = \begin{pmatrix} 1 + 2\alpha_0^+v^+(t) + \alpha_1^+v^-(t) & \alpha_1^+v^+(t) + 2\alpha_2^+v^-(t) \\ \alpha_1^-v^-(t) + 2\alpha_2^-v^+(t) & 1 + 2\alpha_0^-v^-(t) + \alpha_1^-v^+(t) \end{pmatrix}. \tag{4.8}$$

For simplicity, we do not write the explicit form of $w^+(t)$ and $w^-(t)$, but we note that they contain $v^+(t)$ and $v^-(t)$ at least in first order. Thus we obtain from (4.7)

$$\frac{d}{dt}\begin{pmatrix} v^+(t) \\ v^-(t) \end{pmatrix} = M^{-1}(t)\begin{pmatrix} w^+(t) \\ w^-(t) \end{pmatrix}, \tag{4.9}$$

with the inverse matrix

$$M(t)^{-1} = \frac{1}{\operatorname{Det} M(t)}\begin{pmatrix} M_{22}(t) & -M_{12}(t) \\ -M_{21}(t) & M_{11}(t) \end{pmatrix}, \tag{4.10}$$

where the determinant has the form

$$\begin{aligned} \operatorname{Det} M(t) &= 1 + v^+(t)\left(2\alpha_0^+ + \alpha_1^-\right) \\ &+ 2v^+(t)v^-(t)\left(\alpha_0^+\alpha_0^- - \alpha_2^+\alpha_2^-\right) + 2v^+(t)^2\left(\alpha_0^+\alpha_1^- - \alpha_1^+\alpha_2^-\right) + \text{c.c.} \end{aligned} \tag{4.11}$$

Expanding the right-hand side of (4.9) in powers of $v^+(t)$ and $v^-(t)$ up to the third order, we yield

$$\begin{aligned}\frac{d}{dt}v^{\pm}(t) &= \lambda^{\pm}v^{\pm}(t) \\ &+ \left(q_1^{\pm} - \alpha_0^{\pm}\lambda^{\pm}\right)v^{\pm}(t)^2 + \left(q_0^{\pm} - \alpha_1^{\pm}\lambda^{\mp}\right)v^{+}(t)v^{-}(t) + \left[q_2^{\pm} + \alpha_2^{\pm}(\lambda^{\pm} - 2\lambda^{\mp})\right]v^{\mp}(t)^2 \\ &+ \Big[k_1^{\pm} + q_0^{\pm}(\alpha_1^{\mp} - \alpha_0^{\pm}) - q_0^{\mp}\alpha_1^{\pm} + q_1^{\pm}\alpha_1^{\pm} + 2q_2^{\pm}\alpha_2^{\mp} - 2q_2^{\mp}\alpha_2^{\pm} + \alpha_1^{\pm}\alpha_1^{\mp}\lambda^{\pm} \\ &+ 2\alpha_2^{\pm}\alpha_2^{\mp}(2\lambda^{\pm} - \lambda^{\mp}) + \alpha_0^{\pm}\alpha_1^{\pm}(\lambda^{\pm} + 2\lambda^{\mp})\Big]v^{\pm}(t)^2v^{\mp}(t).\end{aligned} \tag{4.12}$$

Now we can fix the yet-unknown coefficients $\alpha_0^{\pm}$, $\alpha_1^{\pm}$, and $\alpha_2^{\pm}$ of the near identity transformation (4.6) in such a way that all quadratic terms vanish. This leads to the conditions

$$\alpha_0^{\pm} = \frac{q_0^{\pm}}{\lambda_u^{\pm}}, \quad \alpha_1^{\pm} = \frac{q_1^{\pm}}{\lambda_u^{\mp}}, \quad \alpha_2^{\pm} = \frac{q_2^{\pm}}{2\lambda_u^{\mp} - \lambda_u^{\pm}}. \tag{4.13}$$

Thus (4.12) reduces to the normal form of a Hopf bifurcation

$$\frac{d}{dt}v^{\pm}(t) = \lambda_u^{\pm}v^{\pm}(t) + b^{\pm}v^{\pm}(t)^2v^{\mp}(t), \tag{4.14}$$

where the Hopf parameter $b^{\pm}$ is given by

$$b^{\pm} = k_1^{\pm} + \frac{q_0^{\pm}q_1^{\pm}(4\lambda_u^{\pm 2} - \lambda_u^{\mp 2}) + q_1^{\pm}q_1^{\mp}(2\lambda_u^{\pm}\lambda_u^{\mp} - \lambda_u^{\mp 2}) + 2q_2^{\pm}q_2^{\mp}\lambda_u^{\pm}\lambda_u^{\mp}}{\lambda_u^{\pm}\lambda_u^{\mp}(2\lambda_u^{\pm} - \lambda_u^{\mp})}. \tag{4.15}$$

Taking into account (2.18), (2.19), (2.23), and (2.32) as well as (3.12), (3.13), (3.18), and (3.19) together with (4.2)–(4.6), this Hopf parameter $b^{\pm}$ reads in the vicinity of the instability as

$$b^{\pm} = -\frac{R_c}{5(1+R_c^2)^{\frac{3}{2}}}\left[(3R_c - 1) \pm i(R_c + 3)\right] + \mathcal{O}(\varepsilon). \tag{4.16}$$

Performing the ansatz

$$v^{\pm}(t) = r(t)e^{\pm i\varphi(t)}, \tag{4.17}$$

the normal form (4.14) is transformed to polar coordinates

$$\frac{d}{dt}r(t) = r(t)\left[\Re\left(\lambda_u^{\pm}\right) + \Re\left(b^{\pm}\right)r(t)^2\right], \tag{4.18}$$

$$\frac{d}{dt}\varphi(t) = \pm\left[\Im\left(\lambda_u^{\pm}\right) + \Im\left(b^{\pm}\right)r(t)^2\right]. \tag{4.19}$$

Thus, taking into account (2.19) and (4.16) near the instability, the oscillatory solution results in

$$r_{\text{stat}} = \sqrt{-\frac{\Re\left(\lambda_u^{\pm}\right)}{\Re\left(b^{\pm}\right)}} = \sqrt{\frac{5R_c}{3R_c - 1}}\sqrt[4]{1+R_c^2}\sqrt{\varepsilon} + \mathcal{O}(\varepsilon), \tag{4.20}$$

$$\frac{d}{dt}\varphi(t) = \pm\left[\Im\left(\lambda_u^{\pm}\right) + \Im\left(b^{\pm}\right)r_{\text{stat}}^2\right] = R_c - \frac{R_c}{3R_c - 1}\varepsilon + \mathcal{O}\left(\varepsilon^2\right). \tag{4.21}$$

In order to compare this result with numerical simulations, we have to convert this oscillatory solution back to the original state space Γ. At first we observe that we obtain, for $z_t \in \mathcal{C}$ from (2.22), (2.35), (3.6), and (3.9) near the instability,

$$z_t(\Theta) = \sum_{j=\pm} \phi^{\lambda_u^j}(\Theta) u^j(t) + \sum_{j_1=\pm} \sum_{j_2=\pm} H_{j_1 j_2}(\Theta) u^{j_1}(t) u^{j_2}(t). \tag{4.22}$$

Taking into account the near identity transformation (4.6) together with (2.23), this yields up to the first order in ε

$$\begin{aligned} z_t(\Theta) = {} & N_{\lambda_u^+} e^{\lambda_u^+ \Theta} v^+(t) + N_{\lambda_u^-} e^{\lambda_u^- \Theta} v^-(t) \\ & + a_0(\Theta) v^+(t)^2 + a_1(\Theta) v^+(t) v^-(t) + a_2(\Theta) v^-(t)^2, \end{aligned} \tag{4.23}$$

where the coefficients $a_0(\Theta)$, $a_1(\Theta)$, $a_2(\Theta)$ read as

$$a_0(\Theta) = \left[N_{\lambda_u^+} e^{\lambda_u^+ \Theta} \alpha_0^+ + N_{\lambda_u^-} e^{\lambda_u^- \Theta} \alpha_2^- + H_{++}(\Theta) \right], \tag{4.24}$$

$$a_1(\Theta) = \left[N_{\lambda_u^+} e^{\lambda_u^+ \Theta} \alpha_1^+ + N_{\lambda_u^-} e^{\lambda_u^- \Theta} \alpha_1^- + H_{+-}(\Theta) + H_{-+}(\Theta) \right], \tag{4.25}$$

$$a_2(\Theta) = \left[N_{\lambda_u^+} e^{\lambda_u^+ \Theta} \alpha_2^+ + N_{\lambda_u^-} e^{\lambda_u^- \Theta} \alpha_0^- + H_{--}(\Theta) \right]. \tag{4.26}$$

Due to the relation (2.2) between $z(t) \in \Gamma$ and $z_t \in \mathcal{C}$, we conclude from (4.23) that

$$\begin{aligned} z(t) = {} & N_{\lambda_u^+} v^+(t) + N_{\lambda_u^-} v^-(t) \\ & + a_0(0) v^+(t)^2 + a_1(0) v^+(t) v^-(t) + a_2(0) v^-(t)^2. \end{aligned} \tag{4.27}$$

Near the instability, we obtain from (2.32)

$$N_{\lambda_u^\pm} = \frac{1}{\sqrt[4]{1+R_c^2}} e^{\pm i \psi_1} + \mathcal{O}(\varepsilon) \tag{4.28}$$

with some phase ψ_1, whereas (4.17)–(4.19) lead to

$$v^\pm(t) = r_{\text{stat}} e^{\pm i \varphi(t)} \tag{4.29}$$

with the radius (4.20) and the phase

$$\varphi(t) = \Omega(\varepsilon) t + \varphi_0. \tag{4.30}$$

Here the frequency turns out to be

$$\Omega(\varepsilon) = R_c - \frac{R_c}{3R_c - 1} \varepsilon. \tag{4.31}$$

Furthermore, we yield from (4.24)–(4.26), by taking into account (3.12), (3.13), (3.18), (3.19), and (4.28) in the lowest order of ε,

$$a_0(0) = \frac{1}{\sqrt{5(1+R_c^2)}} e^{i\psi_2}, \quad a_1(0) = 0, \quad a_2(0) = \frac{1}{\sqrt{5(1+R_c^2)}} e^{-i\psi_2}, \tag{4.32}$$

where ψ_2 denotes some phase. Thus we obtain the following result for $z(t) \in \Gamma$ near the instability:

$$z(t) = c_0(\varepsilon) + c_1(\varepsilon)\cos\left[\varphi(t) + \psi_1\right] + c_2(\varepsilon)\cos\left[2\varphi(t) + \psi_2\right] + \mathcal{O}\left(\varepsilon^{\frac{3}{2}}\right), \tag{4.33}$$

where the respective coefficients read as

$$c_0(\varepsilon) = 0, \quad c_1(\varepsilon) = 2\sqrt{\frac{5R_c}{3R_c - 1}}\sqrt{\varepsilon}, \quad c_2(\varepsilon) = 2\,\frac{\sqrt{5}R_c}{3R_c - 1}\varepsilon. \tag{4.34}$$

Now we compare the oscillatory solution (1.7), (1.8), which was obtained by using the method of averaging, with ours, (4.30), (4.31), (4.33), (4.34), by taking into account the critical value (1.6) of the control parameter. We conclude that both results coincide in the lowest order $\varepsilon^{1/2}$, but our result is even correct up to the order ε.

From the near identity transformation (4.6) as well as from (4.20) and (4.29), we conclude that the order parameters $u^{\pm}(t)$ turn out to be of the order $\varepsilon^{1/2}$. This result is consistent with our original assumption (3.8), which was the basis of our approximate solution of the implicit equation for the center manifold (3.7) in the vicinity of the instability. Thus our synergetic system analysis is justified a posteriori by self-consistency.

Note that the same perturbative result (4.30), (4.31), (4.33), (4.34) for the oscillatory solution above the Hopf bifurcation can be derived with the multiple scale method [10]. It represents a technical procedure to deduce the normal form, once the bifurcation type is known, by using the knowledge of how the respective quantities depend on the smallness parameter $\varepsilon = (R - R_c)/R_c$. Although the multiple scale method was originally developed for ordinary differential equations [24, 25, 26], it can be also applied to delay differential equations (see, for instance, the treatment in [27]).

5. Numerical investigation. In order to numerically verify our analytical result, we integrated the underlying delay differential equation of Wright (1.5). By doing so, we varied the control parameter R in the vicinity of the instability $R_c = \pi/2$ in such a way that the smallness parameter $\varepsilon = (R - R_c)/R_c$ took 200 equidistant values between 10^{-5} and 10^{-1}. We used a Runge–Kutta–Verner method of the IMSL library as an integration routine with a step-size of 10^{-3} and performed a linear interpolation between the respective values in the memory interval. In particular, in the immediate vicinity of the instability, the phenomenon of critical slowing down led to a transient behavior. To exclude this, we iterated the discretized delay differential equation for each value of the control parameter at least 10^6 times. Afterward, we calculated the power spectrum with a complex fast Fourier transform (FFT) so that the basic frequency Ω of the oscillatory solution could be determined with high resolution. Then we performed a real FFT with the period $T = 2\pi/\Omega$ of the simulated periodic signal $z(t) = z(t + T)$:

$$z(t) = \frac{a_0}{2} + \sum_{k=1}^{\infty}\left[a_k\cos\left(k\Omega t\right) + b_k\sin\left(k\Omega t\right)\right]. \tag{5.1}$$

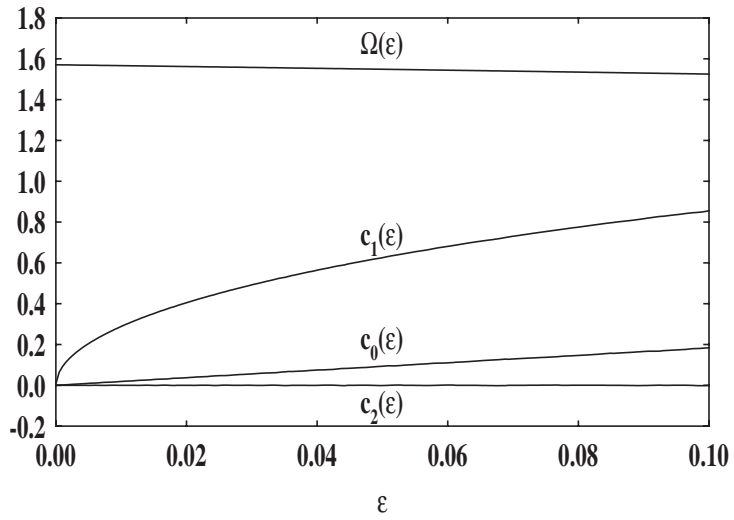

Figure 5.1. *Frequency Ω and Fourier coefficients c_0, c_1, c_2 of the oscillatory solution of the Wright equation after the Hopf bifurcation versus the smallness parameter $\varepsilon = (R - R_c)/R_c$.*

The Fourier coefficients follow from integrations with respect to one period $T = 2\pi/\Omega$:

$$a_k = \frac{2}{T}\int_0^T f(t)\cos(k\Omega t)\,dt, \quad k = 0, 1, \ldots, \infty; \tag{5.2}$$

$$b_k = \frac{2}{T}\int_0^T f(t)\sin(k\Omega t)\,dt, \quad k = 1, \ldots, \infty. \tag{5.3}$$

From (5.1) follows then the spectral representation

$$z(t) = c_0 + \sum_{k=1}^{\infty} c_k \cos(k\Omega t + \phi_k) \tag{5.4}$$

with the quantities

$$c_0 = \frac{a_0}{2}, \quad c_k = \sqrt{a_k^2 + b_k^2}, \quad \phi_k = -\arctan\frac{b_k}{a_k}, \quad k = 1, \ldots, \infty. \tag{5.5}$$

Thus our analytical result (4.30), (4.33) can be interpreted as the first terms within a spectral representation (5.4), where the frequency $\Omega = 2\pi/T$ and the Fourier coefficients c_0, c_1, c_2 are given by (4.31) and (4.34). Numerically analyzing the Hopf bifurcation with the FFT, the results for Ω, c_0, c_1, c_2 are plotted in Figure 5.1 versus the smallness parameter ε. Comparing the respective numerical and analytical results, we observe some deviations for small and for large values of the smallness parameter ε. The former are due to the phenomenon of critical slowing down (i.e., the system stays longer in the transient state when the instability is approached), and the latter arise from the neglected higher-order corrections in the analytical approach. Therefore, we restricted our numerical analysis to the intermediate interval

Table 5.1

Plotting the analytical and numerical values for the frequency $\Omega(\varepsilon)$ and the Fourier coefficients $c_0(\varepsilon)$, $\ln c_1(\varepsilon)$, $c_2(\varepsilon)$ of the oscillatory solution of the Wright equation after the Hopf bifurcation versus ε, we obtain straight lines whose axes intercept and whose slopes are determined.

Quantity	Analytical expression		Analytical value		Numerical value	
	Intercept	Slope	Intercept	Slope	Intercept	Slope
$\Omega(\varepsilon)$	R_c	$\dfrac{R_c}{3R_c-1}$	1.5708	−0.4231	1.5707	−0.4024
$c_0(\varepsilon)$	0	0	0.0	0.0	$-2\cdot10^{-4}$	$4\cdot10^{-2}$
$\ln c_1(\varepsilon)$	$\dfrac{1}{2}\ln\dfrac{20R_c}{3R_c-1}$	$\dfrac{1}{2}$	1.06781	0.5	1.06126	0.4999
$c_2(\varepsilon)$	0	$2\dfrac{\sqrt{5}R_c}{3R_c-1}$	0.0	1.8923	$2\cdot10^{-4}$	1.832

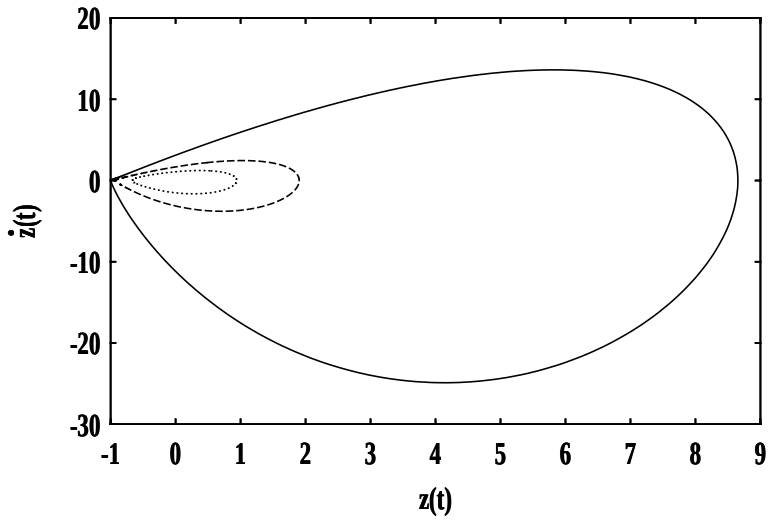

Figure 5.2. *Oscillatory solutions of the Wright equation* (1.5) *for three values of the control parameter R:* 1.7 *(dotted line),* 2.0 *(dashed line), and* 3.247 *(solid line).*

$[10^{-5}, 10^{-1}]$ of the smallness parameter ε. In Table 5.1, we see that the analytically and numerically determined quantities agree quantitatively very well. Thus our synergetic system analysis for the delay-induced Hopf bifurcation in the Wright equation is numerically verified.

For the sake of completeness, we have also investigated oscillatory solutions for values of the control parameter R which are larger than the critical one $R_c = \pi/2$. Figure 5.2 shows that all these periodic solutions oscillate around the stationary state $z^{\mathrm{I}}_{\mathrm{stat}} = 0$, which becomes unstable at $R_c = \pi/2$. It turns out that a global bifurcation occurs for $R^g_c = 3.247$ as then the

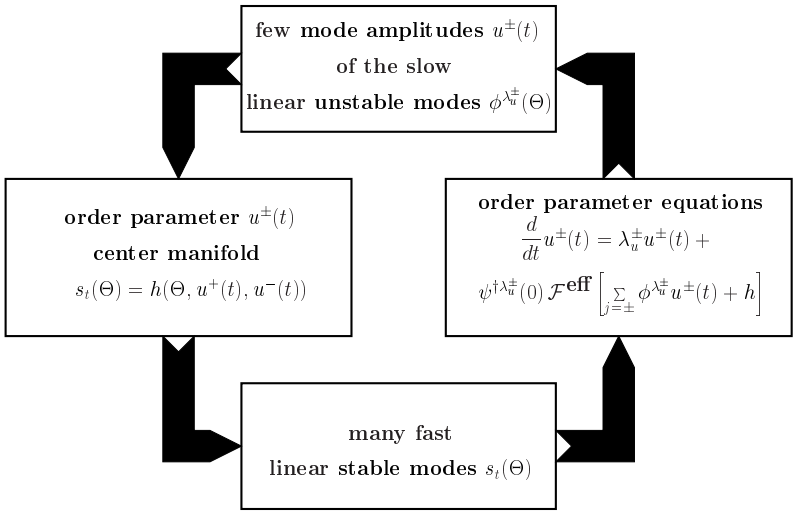

Figure 6.1. *Circular causality chain of synergetics for the Hopf bifurcation of a delay differential equation. On the one hand, the center manifold of the slaving principle guarantees that many fast linear stable modes $s_t(\Theta)$ quasi-instantaneously take values which are prescribed by the few slow linear unstable modes $u^{\pm}(t)$. On the other hand, the adiabatic elimination of the fast enslaved modes $s_t(\Theta)$ influences the resulting order parameter equation.*

oscillatory solution comes close to the other stationary state $z^{\mathrm{II}}_{\mathrm{stat}} = -1$, which turns out to be linear unstable for all values of the control parameter $R > 0$. Indeed, performing a linear stability analysis according to section 2 around the stationary state $z^{\mathrm{II}}_{\mathrm{stat}} = -1$ leads to the characteristic equation

$$R - \lambda = 0, \tag{5.6}$$

so we have from (2.16) the identification $p = R$ and $q = 0$. (Compare this with the shaded stability region in Figure 2.1.)

6. Summary and outlook. In this article, a linear stability analysis of the Wright equation (1.5) around the stationary state $z^{\mathrm{I}}_{\mathrm{stat}} = 0$ showed that a delay-induced Hopf bifurcation occurs at the critical value $R_c = \pi/2$ of the control parameter R. Within a subsequent nonlinear synergetic analysis, we adiabatically eliminated the stable modes and derived the normal form of this Hopf bifurcation. It is explicitly influenced by the center manifold in the lowest order, as the Wright equation (1.5) has a quadratic nonlinearity. Solving the normal form, we obtained a periodic solution above the Hopf bifurcation which was numerically verified.

In contrast to the corresponding analysis of the electronic system of a first-order PLL with time delay [11], this paper not only confirms the order parameter concept for delay systems but also represents a successful test for the slaving principle of synergetics, i.e., for the influence of the center manifold on the order parameter equations. Thus the validity of the circular causality chain of synergetics (see Figure 6.1) has been demonstrated for the Hopf bifurcation of a delay differential equation.

It remains to investigate the circular causality chain for other bifurcations. For instance,

it may be interesting to revisit a Hopf bifurcation of codimension two in delayed systems as it occurs in some robotics applications [28]. Furthermore, the Floquet theory for delay differential equations, and thus the linear stability analysis for a periodic reference state, was already established in [29, 30, 31]. However, a corresponding synergetic system analysis which derives the order parameter equations and the normal forms for bifurcations of oscillatory solutions is still missing [10, 11, 32].

Acknowledgments. We are thankful to Michael Bestehorn and Rudolf Friedrich for contributing various useful comments at an initial stage of this work. Furthermore, we thank Hermann Haken and Arne Wunderlin for teaching us synergetics for many years. Finally, Axel Pelster is grateful for the hospitality of Günter Wunner at the I. Institute of Theoretical Physics at the University of Stuttgart as this article was finished there.

REFERENCES

[1] H. Haken, *Synergetics: An Introduction*, 3rd ed., Springer-Verlag, Berlin, 1983.
[2] H. Haken, *Advanced Synergetics*, corrected second printing, Springer-Verlag, Berlin, 1987.
[3] H. Haken, *Information and Self-Organization*, Springer-Verlag, Berlin, 1988.
[4] H. Haken, *Synergetic Computers and Cognition*, Springer-Verlag, Berlin, 1991.
[5] H. Haken, *Principles of Brain Functioning*, Springer-Verlag, Berlin, 1996.
[6] I. Grabec and W. Sachse, *Synergetics of Measurements, Prediction, and Control*, Springer Ser. Synergetics 68, Springer-Verlag, Berlin, 1997.
[7] W. Wischert, A. Wunderlin, A. Pelster, M. Olivier, and J. Groslambert, *Delay-induced instabilities in nonlinear feedback systems*, Phys. Rev. E (3), 49 (1994), pp. 203–219.
[8] J. K. Hale, *Theory of Functional Differential Equations*, 2nd ed., Springer-Verlag, New York, 1977.
[9] N. Krasovskii, *Stability of Motion*, Stanford University Press, Stanford, CA, 1963.
[10] M. Schanz, *Zur Analytik und Numerik zeitlich verzögerter synergetischer Systeme*, Dissertation, Universität Stuttgart, Stuttgart, Germany, 1997.
[11] M. Schanz and A. Pelster, *Analytical and numerical investigations of the phase-locked loop with time delay*, Phys. Rev. E, 67 (2003), 056205.
[12] G. Stépán, *Great delay in a predator-prey model*, Nonlinear Anal., 10 (1986), pp. 913–929.
[13] G. Stépán and T. Kalmár-Nagy, *Nonlinear regenerative machine tool vibrations*, in Proceedings of the 16th ASME Biennial Conference on Mechanical Vibration and Noise, S. C. Sinha, ed., Sacramento, CA, 1997, pp. 1–11.
[14] T. Kalmár-Nagy, G. Stépán, and F. C. Moon, *Subcritical Hopf bifurcation in the delay equation model for machine tool vibrations*, Nonlinear Dynam., 26 (2001), pp. 121–142.
[15] P. F. Verhulst, *Notice sur la loi que la population suit dans son accroissement*, Corr. Math. Phys., 10 (1838), pp. 113–121.
[16] F. Verhulst, *Nonlinear Differential Equations and Dynamical Systems*, Springer-Verlag, New York, 1990.
[17] E. M. Wright, *A non-linear difference-differential equation*, J. Reine Angew. Math., 194 (1955), pp. 66–87.
[18] W. J. Cunningham, *A nonlinear differential-difference equation of growth*, Proc. Nat. Acad. Sci. U.S.A., 40 (1954), pp. 708–713.
[19] J. E. Marsden and M. McCracken, *The Hopf Bifurcation and Its Applications*, Appl. Math. Sci. 19, Springer-Verlag, New York, 1976.
[20] N. D. Hayes, *Roots of the transcendental equation associated with a certain difference-differential equation*, J. London Math. Soc., 25 (1950), pp. 226–232.
[21] J. Guckenheimer and P. Holmes, *Nonlinear Oscillations, Dynamical Systems and Bifurcations of Vector Fields*, Appl. Math. Sci. 42, Springer-Verlag, New York, 1992.

[22] R. H. Rand and D. Armbruster, *Perturbation Methods, Bifurcation Theory and Computer Algebra*, Appl. Math. Sci. 65, Springer-Verlag, New York, 1987.

[23] P. Tass, A. Wunderlin, and M. Schanz, *A theoretical model of sinusoidal forearm tracking with delayed visual feedback*, J. Biol. Phys., 21 (1995), pp. 83–112.

[24] J. Kevorkian, *The two-variable expansion procedure of the approximate solution of certain nonlinear differential equations*, in Space Mathematics (Proc. Summer Seminar, Ithaca, NY, 1963), Part 3, AMS, Providence, RI, 1966, pp. 206–275.

[25] W. Lick, *Two-variable expansions and singular perturbation problems,* SIAM J. Appl. Math., 17 (1969), pp. 815–825.

[26] A. Wunderlin and H. Haken, *Scaling theory for nonequilibrium systems*, Z. Phys. B, 21 (1975), pp. 393–401.

[27] E. Grigorieva, H. Haken, S. A. Kashchenko, and A. Pelster, *Travelling waves dynamics in nonlinear interferometer with spatial field transformer in feedback*, Phys. D, 125 (1999), pp. 123–141.

[28] G. Stépán and G. Haller, *Quasiperiodic oscillations in robot dynamics*, Nonlinear Dynam., 8 (1995), pp. 513–528.

[29] C. Simmendinger, O. Hess, and A. Wunderlin, *Analytical treatment of delayed feedback control*, Phys. Lett. A, 245 (1998), pp. 253–258.

[30] C. Simmendinger, A. Wunderlin, and A. Pelster, *Analytical approach for the Floquet theory of delay differential equations*, Phys. Rev. E (3), 59 (1999), pp. 5344–5353.

[31] T. Insperger and G. Stépán, *Stability chart for the delayed Mathieu equation*, R. Soc. Lond. Proc. Ser. A Math. Phys. Eng. Sci., 458 (2002), pp. 1989–1998.

[32] M. Schanz and A. Pelster, *On the period-doubling scenario in dynamical systems with time delay*, in Proceedings of the 15th IMACS World Congress on Scientific Computation, Modeling and Applied Mathematics, Berlin, 1997, Wissenschaft und Technik Verlag, 1 (1997), pp. 215–220.